Avestia Publishing
Journal Name: Journal of Fluid Flow, Heat and Mass Transfer (JFFHMT)
Volume 12, Year 2025
ISSN: 2368-6111
DOI: 10.11159/jffhmt.2025.040

Stagnation-Point Flow of Williamson Fluid: A Study on Dual Solutions and Stability Analysis

Dibjyoti Mondal[1], Abhijit Das[1]
[1] Department of Mathematics, National Institute of Technology Tiruchirappalli,
Tiruchirappalli, Tamil Nadu-620015, India
dibjyoti002121@gmail.com

Abstract - Since non-Newtonian fluids are often encountered in engineering devices, the nonlinear boundary layer equations governing the flow and heat transfer properties of a non-Newtonian Williamson fluid over a stretching $(c > 0)$ or shrinking $(c < 0)$ sheet near the stagnation point are analyzed using two closely interrelated approaches. First, employing the shooting argument, it is proved that a unique solution exists when $c \in (-1, \infty)$ and second, using the BVP4C solver in MATLAB, two different solution branches are reported on the interval $[c_T, -1]$, where c_T is the bifurcation point. The c_T values become more negative with increasing values of the Williamson parameter λ, marking the broadening of the solution range. Furthermore, the first solution branch continues for large positive values of c, whereas the second branch seems to cease at $F''(0) = 0$ as $c \to -1$. The smallest eigenvalue computed using temporal stability analysis of these solutions is found to be positive for the first branch, indicating that this branch is physically stable. These findings are relevant to various industrial processes involving non-Newtonian fluids, such as polymer processing and coating applications. Finally, an asymptotic expression is derived to provide insights into the behavior of large c.

Keywords: Williamson fluid, Existence-Uniqueness, Dual solutions, Stability analysis, Asymptotic analysis.

1. Introduction

It is common knowledge that many industrial (such as paints and coatings) and physiological (such as blood and plasma) fluids exhibit complex flow behavior that the classical Newtonian fluid model cannot adequately describe. To gain a better understanding of such fluids, numerous models (non-Newtonian) have been suggested over the years to take into account the unique characteristics of these fluids, including their viscoelastic properties, shear-thinning or shear-thickening behavior, and time-dependent responses [1, 2]. The nonlinear relationships between the stress tensor and the deformation rate tensor for non-Newtonian fluids give rise to complex equations. Undoubtedly, it is challenging to prove the existence and uniqueness/non-uniqueness of a solution to these equations and obtain their numerical solution.

This paper focuses on the robust model put forward by Williamson to describe pseudoplastic fluids [3]. A large number of published works, for example, the study of the flow of a thin layer of pseudoplastic fluid over an inclined solid surface [4], the peristaltic flow of chyme in the small intestine [5], blood flows through a tapered artery with stenosis [6], and some boundary layer flows of Williamson fluid [7], to mention a few, demonstrate the adequacy of Williamson's model in describing many frequently observed industrial and physiological fluids like polymer solutions, paints, blood, and plasma. Further, one can go through the investigations [8, 9] for Williamson fluid flows in various geometries (especially stagnation point flow and stretching/shrinking surface) under diverse physical conditions. Due to its immense engineering and industrial applications, the stagnation-point flow of a viscous or non-Newtonian fluid has been the subject of several investigations [10, 11]. Another significant aspect of boundary layer flow involves the stretching or shrinking phenomena [12].

A review of the literature suggests that the flow generated by a shrinking sheet has recently captured the

Date Received: 2025-01-23
Date revised: 2025-09-25
Date Accepted: 2025-10-09
Date Published: 2025-12-01

Nomenclature

V	Velocity vector
T	Temperature
B	First Rivlin-Erickson tensor
P	Pressure
K	Thermal conductivity
c_p	Specific heat
C	Stretching/ Shrinking
Pr	Prandtl number
λ	Non-Newtonian parameter
C_F	Skin friction coefficient
Nu_x	Nusselt number
τ	Anisotropic viscous stress tensor

interest of researchers due to its intriguing physical characteristics and growing practical implementations. Wang [11] introduced the concept of flow resulting from a shrinking sheet and showed that the solution is not unique to a particular domain. Subsequently, several research papers [13-15] have been published addressing the shrinking sheet problem. The works mentioned above were devoted to finding multiple solutions and their stability analysis. Analyzing multiple solutions and stability is crucial in engineering analysis as it enables the determination of the physical relevance of a steady-state solution. In the context of stability analysis, Merkin [16] first found that in time-dependent problems of steady-state flows, only the stable upper branch solution is physically possible, as it has the smallest positive eigenvalue. In contrast, the unstable lower branch solution is not physically relevant. Recent studies in references [17, 18] have discussed the stability of multiple solutions associated with stretching or shrinking surfaces.

In the last few decades, numerous investigations have demonstrated the mathematical proof of the existence and uniqueness of solutions in boundary layer fluid flow problems. Miklavčič and Wang [19] established the existence and uniqueness of the similarity solution for the equation describing the flow caused by a shrinking sheet with suction. Gorder et al. [20] examined the results concerning the existence and uniqueness of solutions over the interval $[0, \infty)$ for the stagnation-point flow of a hydromagnetic fluid over a stretching or shrinking sheet. Pallet et al. [10] proved the existence and uniqueness of a solution for oblique stagnation point flow by using the topological shooting argument. However, to the best of the authors' knowledge, only a limited number of articles are devoted to answering the question of the existence of a unique solution, see [21, 22, 23] and the references therein for a detailed understanding of the methodology used.

Motivated by the investigations mentioned above and recognizing the widespread applications of problems involving stretching/shrinking sheets and non-Newtonian fluids in engineering and industries, we consider the stagnation point flow of the Williamson fluid model over a stretching/shrinking surface here. Primarily, the following research questions are addressed

- How can the existence and uniqueness of solutions for the stretching/shrinking parameter $c > -1$ be mathematically established?
- What is the critical point c_T, and how does the nature of the solution change when $c < c_T$?
- What are the characteristics of dual solutions in the shrinking parameter range $c_T \leq c \leq -1$?
- How can a linear stability analysis be conducted to identify stable solutions?
- What are the effects of the non-Newtonian parameter λ and shrinking parameter c (specifically $c \leq -1$) on the velocity and temperature profiles in the dual solution?
- How do the expressions for shear stresses and the Nusselt number behave for large c ?

2. Flow Analysis

The continuity and momentum equations for an incompressible Williamson fluid are expressed as follows [7]

$$\text{div}\,\mathbf{V} = 0 \quad (1)$$

$$\rho\frac{d\mathbf{V}}{dt} = \text{div}(-p\mathbf{I} + \tau) + \rho\mathbf{f} \quad (2)$$

The energy equation is

$$\rho c_p\left(\frac{\partial T}{\partial t} + \mathbf{V}\cdot\nabla\mathbf{T}\right) = \nabla\cdot k\nabla\mathbf{T} \quad (3)$$

Here, $\mathbf{V}$ represents the velocity vector, $\boldsymbol{T}$ denotes the temperature, ρ stands for density, $\mathbf{f}$ denotes the body force, $\frac{d}{dt}$ signifies the material time derivative, p represents pressure, c_p indicates the specific heat, k represent the thermal conductivity and $\mathbf{I}$ be the identity matrix. τ be anisotropic viscous stress tensor defined as [7]

$$\tau = \left[\mu_\infty + \frac{\mu_0 - \mu_\infty}{1 - \Gamma\gamma}\right]\mathbf{B}. \quad (4)$$

Here μ_0 and μ_∞ be zero and infinity shear rate viscosity, respectively, $\mathbf{B}$ be the first Rivlin-Erickson tensor, Γ be the time constant and γ is defined as

$$\gamma = \sqrt{\frac{1}{2}\text{trace}(\mathbf{B}^2)} \quad (5)$$

As in [7], we investigate the circumstance where $\mu_\infty = 0$ and $\Gamma\gamma < 1$. Under this variation, (4) transforms into

$$\tau = \mu_0[1 + \Gamma\gamma]\mathbf{B} \quad (6)$$

Consider a steady, two-dimensional, incompressible flow of a Williamson fluid over a horizontal linearly stretching/shrinking sheet with no body force. The sheet, which coincides with the plane $y = 0$, is assumed to be impermeable, so there is no normal velocity across its surface. The flow is restricted to the area where $y > 0$. The sheet's velocity is represented by $u_w(x) = p_1 x$, where $u_e(x) = bx$ (where $b > 0$) characterizes the free stream velocity. Here, the constant $p_1 > 0$ represents stretching and $p_1 < 0$ represents shrinking. Let (u, v) be the velocity component in (x, y) direction and T be the temperature. Following [7], the boundary layer equations are expressed as

$$\left(u\frac{\partial u}{\partial x} + v\frac{\partial u}{\partial y}\right) = \frac{\mu_0}{\rho}\left(\frac{\partial^2 u}{\partial y^2} + 2\Gamma\frac{\partial u}{\partial y}\frac{\partial^2 u}{\partial y^2}\right) - \frac{1}{\rho}\frac{\partial p}{\partial x}, \quad (7)$$

and

$$\left(v\frac{\partial T}{\partial y} + u\frac{\partial T}{\partial x}\right) = \frac{k}{\rho c_p}\frac{\partial^2 T}{\partial y^2}. \quad (8)$$

Relevant boundary conditions for the stagnation point flow of Williamson fluid over a stretching/shrinking sheet [7] are

$$(u, v, T) = (u_w, 0, T_w) \text{ at } y = 0, \quad (9)$$

$$(u, T) \to (u_e, T_\infty) \text{ as } y \to \infty, \quad (10)$$

where T_w and T_∞ are the surface and ambient temperature, respectively. Using the Bernoulli equation and neglecting the hydrostatic term, $-\frac{1}{\rho}\frac{\partial p}{\partial x} = u_e\frac{du_e}{dx}$, gives $-\frac{1}{\rho}\frac{\partial p}{\partial x} = b^2 x$.

Following the similarity transformations

$$u = bxF'(s), v = -\sqrt{b\nu}F(s), T = T_w + (T_w - T_\infty)\zeta(s)$$

[7], where $s = \sqrt{\frac{b}{\nu}}y$,

the equations (7)-(8) become

$$F''' - F^2 + 1 + FF'' + \lambda F''F''' = 0, \quad (11)$$

$$\zeta'' + \text{Pr}F\zeta' = 0, \quad (12)$$

where $\lambda = 2\Gamma x\sqrt{\frac{b^3}{\nu}}$ be the non-Newtonian Williamson parameter and $\text{Pr} = \frac{\nu\rho c_p}{k}$ is the Prandtl number. Also, the boundary conditions (9)-(10) become

$$F(0) = 0, F'(0) = c, F'(\infty) \to 1, \zeta(0) = 1, \ \zeta(\infty) \to 0, \quad (13)$$

where $c = \frac{p_1}{b}$ represents the stretching $(c > 0)$ or shrinking $(c < 0)$ parameter. Wall suction and injection effects are neglected in this study $(F(0) = 0)$.

The coefficient of skin friction C_F and the Nusselt number Nu_x, which are two crucial physical parameters, are outlined below

$$C_F = \frac{\tau_{xy}\big|_{y=0}}{\rho u_e^2}, Nu_x = \frac{xQ_w}{k(T_w - T_\infty)}. \quad (14)$$

Here, τ_{xy} represents the skin friction or shear stress along the stretching/shrinking surface, and Q_w denotes the heat flux originating from the stretching/shrinking surface. These quantities are specified as follows

$$\tau_{xy} = \mu_0 \left(\frac{\partial u}{\partial y} + \Gamma \left(\frac{\partial u}{\partial y} \right)^2 \right),$$

$$Q_w = -k \left(\frac{\partial T}{\partial y} \right) |_{y=0}.$$

After using the similarity transformation, equation (14) becomes

$$Re^{\frac{1}{2}} C_F = F''(0) + \frac{\lambda}{2} F''(0)^2,$$

$$Re^{-\frac{1}{2}} Nu_x = -\zeta'(0), \qquad (15)$$

where $Re = \sqrt{\frac{bx^2}{\nu}}$ is the Reynolds number.

3. Existence and uniqueness results for $c > -1$

3.1 Existence for $F(s)$

The existence of a solution for the boundary value problem in equations (11)-(13) is analyzed using the topological shooting method. This method entails the investigation of a corresponding group of initial value problems (IVP), denoted as the ODEs (11) and (13) (except the condition at ∞), in conjunction with an additional initial condition specified as $F''(0) = a$, where a can take any arbitrary values. Then, the solution of the IVP depends on both s and a and is denoted as $F(s; a)$. Although each a yields a solution for the IVP, not all these solutions will satisfy the boundary conditions (13). Therefore, it is necessary to determine a suitable value for a that satisfies the condition at ∞. To prove the existence of a solution, the range $c > -1$ is divided into two parts: $-1 < c \leq 1$ and $c > 1$. For $c = 1$, the identity function $F(s) = s$ is a solution of (11). In this case $F''(0) = a = 0$ for all s, therefore, we did not consider the case $c = 1$ in our proof.

3.1.1 Existence Proof for $-1 < c < 1$

Let us assume two sets P and Q are subsets of $(0, \infty)$, defined by

$$P = \{a > 0: \exists s_1 > 0 \text{ such that } F''(s_1; a) = 0 \text{ and } c < F'(s; a) < 1 \text{ for } s \in (0, s_1]\},$$

$$Q = \{a > 0: \exists s_1 > 0 \text{ such that } F'(s_1; a) = 1 \text{ and } 0 < F''(s; a) < a \text{ for } s \in (0, s_1]\}. \qquad (16)$$

Lemma 1. *P and Q are open sets with no elements in common.*

Proof: Clearly P and Q have no element in common. Let $a_1 \in P$ then $\exists\ s_1 > 0$ such that $F''(s_1; a_1) = 0$ and $c < F'(s; a_1) < 1$ for $s \in (0, s_1]$. Since $F'''(s_1; a_1) = (F'(s_1; a_1))^2 - 1 \neq 0$, therefore, using the property of continuous functions $\exists$ a neighborhood of a_1 such that for all points in the neighborhood, $F'''(s)$ have the same sign as $F'''(s_1; a_1)$. Thus $F''(s)$ has a root with $c < F'(s) < 1$. This shows that P is an open set. Similarly, one can prove that Q is open as well.

Lemma 2. *P is non-void.*

Proof: We claim that when a is very small, it is in P. Let $a = 0$, then $F'''(0; a) < 0$ for all a. Thus, in a small enough vicinity around $s = 0$, it holds that $F''(s; 0) < 0$ and $F'(s, 0) < 1$. Then, through the continuous solutions of the IVP, along with its initial conditions, there is a positive number a for which $F''(s; a) < 0$ and $F'(s; a) < 1$ hold for all values of s in the vicinity of $s = 0$. But $F''(0; a) = a > 0$, implies $\exists$ a $\delta > 0$ such that $F''(\delta; a) = 0$ and $F'(s; a) < 1$ for $s \in (0, \delta]$. Hence for small a (> 0), it is in P.

Lemma 3. *Q is non-void.*

Proof: We claim that when a is very large, it is in Q, that is $F' = 1$ in (0,1] strictly before $F'' = 0$. If this is not the case, then the following possibilities must occur : (i) $F''(s; a) = 0$ for some point in (0,1] for which $F'(s; a) < 1$, (ii) $F''(s; a) > 0$ and $F'(s; a) < 1$ in (0,1], and (iii) $F''(s; a) = 0$ and $F'(s; a) = 1$ occur concurrently. If possible, let $\exists\ c_1 \in (0,1]$ such that $F''(c_1; a) = 0$ with $c_1 < F'(s; a) < 1$ for $s \in (0, c_1]$. By integrating, we get $c_1 s < F(s; a) < s$. Now let $\bar{F} = \int_0^s \frac{F}{1+\lambda F''} dt$ and integrating (11) from 0 to s, we get

$$F''(s)e^{\bar{F}(s)} - F''(0)e^{\bar{F}(0)} = \int_0^s \frac{1-F'^2}{1+\lambda F''}dt, \quad (17)$$

$$\Rightarrow F''(s)e^{\bar{F}(s)} = a + \int_0^s \frac{1-F^2}{1+\lambda F''}dt. \quad (18)$$

Let $H = \frac{1-F'^2}{1+\lambda F''}dt > 0$, then from (18) we have

$$F''(s)e^{\bar{F}(s)} = a + Hs. \quad (19)$$

Then for $s \in (0, c_1]$

$$F''(s) \geq (a+H)e^{-\bar{F}(s)}. \quad (20)$$

Thus, for large a, $F''(s;a) > 0$ for all s, leading to a contradiction. Similarly, it can be shown that the second statement cannot occur for sufficiently large values of a. If the third case occurs, then from (11), we get $F'''(s;a) = 0$. That implies that $F'(s) = 1$, which contradicts the fact that $F'(0) = c \neq 1$. Therefore, sufficiently large a belongs to Q.

Theorem 1. *For any $\lambda \geq 0$, equations (11) and (13) have a solution. Also, the solution is monotone in nature.*

Proof: As $(0,\infty)$ is a connected set, and both P and Q are non-empty, open, and disjoint from each other, it follows from the definition of a connected set that the union of P and Q cannot be equal to $(0,\infty)$. Therefore $\exists\, l > 0$ such that $l \notin P$ and $l \notin Q$. Also, Lemma 3 implies that $F''(s;l) = 0$ and $F'(s;l) = 1$ do not occur simultaneously. Consequently, there is only one possibility that $F''(s;l) > 0$ and $c \leq F'(s;l) < 1\ \forall s$. Now, from equation (11), it is observed that as $F'(\infty;l)$ approaches 1, implies the existence of a monotonically increasing solution to the boundary value problem (11), (13).

3.1.2 Existence Proof for $c > 1$

Let us assume two sets U and V are subsets of $(-\infty, 0)$, defined by

$U = \{a < 0\colon \exists\, s_1' > 0\ \textit{such that}\ F''(s_1';a) = 0\ \textit{and}\ 1 < F'(s;a) < c\ \textit{for}\ s \in (0, s_1']\}$,

$V = \{a < 0\colon \exists\, s_1' > 0\ \textit{such that}\ F'(s_1';a) = 1\ \textit{and}\ c < F''(s;a) < 0\ \textit{for}\ s \in (0, s_1']\}$.

As mentioned in the previous subsection, we will show the same properties (Lemma 1-3) of the sets U and V. To show U and V are open is the same as the previous proof, so we skip this. To prove U is non-void, we will show that if $a < 0$ and $|a|$ is very small, it belongs to U. Now, from (13), first we take $a = 0$ and subsequently, at $s = 0$,

$$F'''(0;0) = (c+1)(c-1) > 0 \text{ as } c > 1, \quad (21)$$

$$F''(0;0) = 0 \text{ and } F'(0;0) = c > 1. \quad (22)$$

So we can say that if s is close to 0 then $F''(s;0) > 0$ and $F'(s;0) > 1$. By continuous solution of the IVP, for $a \neq 0$ with sufficiently small magnitude, it is evident that $F'(s;a)$ will be close to $F'(s;0)$. Specifically, $F'(s;a) > 1$ with $F''(s;a) \geq 0$, but $F''(0;a) < 0$ based on equation (13). This implies that there exists $s_0 > 0$ where $F''(s_0;a) = 0$, and $F'(s;a) > 1$ whenever $s \leq s_0$, showing that the set U is non-empty.

Next, we will prove that V is non-empty. For that, first, we integrate equation (11) from 0 to s which gives

$$F'' = \frac{a - s + 2\int_0^s F'^2 ds - FF' + \lambda \frac{a^2}{2}}{1 + \lambda \frac{F''}{2}}. \quad (23)$$

We claim that for large a, it is in V. If possible, let the statement mentioned above be false, then at least one among the following options is necessary: (i) $F''(s;a) = 0$ at some point in (0,1] with $F'(s;a) > 1$. (ii) $F''(s;a) < 0$ and $F'(s;a) > 1$ for all s in (0,1]. (iii) $F''(s;a) = 0$ and $F'(s;a) = 1$ occurs at the same time. Now, we need to refute each of these statements. Starting with (i), let us assume that $\exists c_2$ such that $F''(c_2;a) = 0$ with $1 < F(s;a) < c$ for $s \leq c_1$. After integrating, we have $s < F'(s;a) < cs$. From (23), we can write

$$F'' \leq \frac{a\left(1 + \frac{a\lambda}{2}\right)}{1 + \frac{\lambda F''}{2}} + \frac{2\int_0^s F^2 ds}{1 + \frac{\lambda F''}{2}}. \quad (24)$$

We are establishing some inequalities to find the bounds of F'' : (a) since $1 + \frac{\lambda a}{2} \geq 1 + \frac{\lambda F''}{2}$, implies that $\frac{a\left(1+\frac{a\lambda}{2}\right)}{1+\frac{\lambda F''}{2}} \leq a$, (b) For $0 < s < 1$ implies that $2\int_0^s F'^2 ds \leq$

$2c^2$, also $\frac{1}{1+\frac{\lambda F''}{2}} \leq 1$ implies that $\frac{2\int_0^s F'^2 ds}{1+\frac{\lambda F''}{2}} \leq 2c^2$. After applying the inequalities (a)-(b) in (24), we have

$$F'' \leq a + 2c^2 \tag{25}$$

Now, if we assume that $a < -2c^2$, then (25) gives $F'' < 0$, which is a contradiction. So (i) can not happen. Similarly, if we take $a < -c - 2c^2$, then (ii) can not happen. If (iii) occurs, then from (13) we have $F''(s) = 0$ implying that $F'(s) = 1$ which contradicts the existence theorem of IVP as $F'(0) = c > 1$. Hence, if $a < -c - 2c^2$, then $F'(s; a) = 1$ before $F''(s; a) = 0$, implies $a \in V$ and V is non-empty.

The sets U and V are non-empty, open, and mutually exclusive. Since $(-\infty, 0)$ is a connected set, therefore $U \cup V \neq (-\infty, 0)$. Hence, there exists a^* that is not in U or V. For that particular value of a^*, the only option is $F''(s; a^*) < 0$ and $1 < F'(s; a^*) < c$ for $s > 0$. Therefore $F'(\infty, a^*) \to m$ (finite). Now, from (11), we get $m = 1$ which completes the proof.

3.1.3 Uniqueness Proof for $-1 < c \leq 1$

Theorem 2. For any $\lambda \geq 0$, the solution is unique.

Proof: We will prove this theorem by using the method of contradiction. Let us assume that $\exists\, a_1,\, a_2$ (values of $F''(0)$) such that $F(s; a_1)$ and $F(s; a_2)$ are the corresponding solutions. Apply MVT on the function F' in the interval $[a_1, a_2]$ and as $s \to \infty$ then $\exists\, a^* \in [a_1, a_2]$ such that $\frac{\partial F'}{\partial a}(\infty, a^*) = 0$. Next, let $\frac{\partial F'}{\partial a} = w'(s; a)$ and differentiating (11) and using the boundary conditions (13), we have

$$w''' - 2F'w' + \lambda(w'''F'' + F'''w'') + (F'w' + Fw'') = 0, \tag{26}$$

with

$$w(0) = 0, w'(0) = 0, w''(0) = 1, w'''(0) = \frac{-\lambda F'''(0)}{1+\lambda a}. \tag{27}$$

Further differentiating (26), we have

$$w^{iv}(1 + \lambda F'') + 2\lambda F'''w''' + \lambda w''F^{iv} - F''w' + Fw'' = 0. \tag{28}$$

Now, from (27), we can say that $\exists\, s_1 > 0$ such that $w'(s; a) > 0, w''(s; a) > 0, w'''(s; a) < 0$ for $s < s_1$. Specifically, the function $w'(s; a)$ is convex downwards, initially increasing, and it has a maximum value to reach zero. Let the maximum value occur at s_2. Consequently, $w'''(s_2; a) = 0$ and $w^{iv}(s; a) \leq 0$ for $s < s_2$. Also, $w^{iv}(s_2) = 0$. But equation (28) implies

$$w^{iv}(s_2) = \frac{1}{1+\lambda F''(s_2)}\big(-2\lambda w'''(s_2)F'''(s_2) + F''(s_2)w'(s_2)\big) > 0, \tag{29}$$

a contradiction. However, up until the point $s_2, w(s; a)$ and all its derivatives up to $w'''(s; a)$ are growing positively. Hence, $F(s; a)$ and all its derivatives up to $F'''(s; a)$ are increasing functions. Therefore, for any a in the interval $[a_1, a_2]$, $w'(s_2, a) \neq 0$ which contradicts the MVT of F'. Hence, the proof is complete.

3.1.4 Uniqueness Proof for $c > 1$

The proof part is similar to Theorem 2. As in Theorem 2, we define w, which satisfies the equation (30) and the boundary conditions $w(0) = 0, w'(0) = 0, w''(0) = 1$. Here, we observe that w and w' are first positive and increasing. Suppose there exist two solutions corresponding to $a_1^* < a_2^* < 0$ (values of $F''(0)$). We first prove that w' cannot have a maximum value. If possible, suppose that w' has a maximum at s_2^* and at this point, we get $w(s_2^*) > 0, w'(s_2^*) > 0, w''(s_2^*) = 0$ and $w'''(s_2^*) < 0$. Moreover, for $s < s_2^*$, we have

$$1 < F'(s; a_1^*) \leq F'(s; a) \leq F'(s; a_2^*) \tag{30}$$

$$F''(s; a_1^*) \leq F''(s; a) \leq F''(s; a_2^*) < 0, \tag{31}$$

Now from (30), we get

$$w'''(s_2^*) = \frac{1}{1 + \lambda F''(s_2^*)}[F'(s_2^*)w'(s_2^*)$$

$$\lambda F'''(s_2^*)w''(s_2^*) - F(s_2^*)w''(s_2^*)] > 0 \tag{32}$$

which contradicts that $w'''(s_2^*) < 0$. Therefore, w' cannot have a maximum, and a positive L and s_3 exists for which w' is greater than L for all s beyond s_3. Applying MVT, we can write for $a_1^* < a^{**} < a_2^*$

$$F'(s; a_2^*) - F'(s; a_1^*) = \left(\frac{\partial F'}{\partial a}\right)_{a=a^{**}} = (a_2^* - a_1^*) \tag{33}$$

As $s \to \infty$ in (33) gives a contradiction (left-hand side is 0 and right-hand side is always positive), demonstrating that for $c > 1$, there cannot be two solutions.

3.2 Existence for $\zeta(s)$:

Theorem 3. If $\zeta(s)$ is a twice differentiable function satisfying (12) with boundary condition (13), then $\zeta(s)$ is of the form

$$\zeta(s) = \frac{\int_s^\infty \left(e^{-\int_0^s PrFds}\right) ds}{\int_0^\infty \left(e^{-\int_0^s PrFds}\right) ds}. \quad [24] \qquad (34)$$

4 Numerical Solution

In this section, we are solving (11)-(13) numerically by the BVP4C solver in MATLAB. Now, equations (11)-(13) can be written as a system of first-order initial value problems. For that let $F = y_1, F' = y_2, F'' = y_3, \zeta = y_4, \zeta' = y_5$ then from (11)-(13), we can obtain

$$\left.\begin{aligned} y_1' &= y_2 \\ y_2' &= y_3 \\ y_3' &= \frac{y_2^2 - y_1 y_3 - 1}{1 + \lambda y_3} \\ y_4' &= y_5 \\ y_5' &= -\mathrm{Pr} y_1 y_5 \end{aligned}\right\} \qquad (35)$$

with

$$\left.\begin{aligned} y_1(0) &= 0 \\ y_2(0) &= c \\ y_2(\infty) &= 1 \\ y_4(0) &= 1 \\ y_4(\infty) &= 0 \end{aligned}\right\} \qquad (36)$$

Now, we can solve equation (35) along with the boundary conditions (36). To obtain the value of s_∞we need to choose initial values and use them to solve for F'', F', F, ζ' and ζ. The MATLAB solver BVP4C was employed with a mesh of 400 points, a relative tolerance of 10^{-6} , and an absolute tolerance of 10^{-8}. The far-field boundary was truncated at $s_\infty = 10$, ensuring that velocity and temperature gradients approached zero. Numerically, it is seen that within a specific range of c, there are two sets of solutions for different values of λ. Determining an initial estimate for the first solution is relatively straightforward, as the BVP4C method converges to the first solution even with suboptimal guesses. However, generating a suitably accurate estimate for the solution becomes challenging in the case of opposing flow. To address this challenge, we initiate the process with a group of parameter values that make the problem easily solvable. Subsequently, we employ the acquired outcome as the initial estimate for solving the problem with slight parameter variations. This process is reiterated until the accurate parameter values are attained.

5 Asymptotic Analysis

To find a solution to equations (11)-(13) for large c, we put

$$F = c^{\frac{1}{2}}\mathcal{F}, \lambda = c^{-\frac{3}{2}}\lambda^*, s = c^{-\frac{1}{2}}\mathcal{Y} \qquad (37)$$

and leaving $\zeta(s)$ unsealed. This gives

$$\mathcal{F}''' + \lambda^*\mathcal{F}''\mathcal{F}''' + \mathcal{F}\mathcal{F}'' - \mathcal{F}'^2 + 1 = 0,$$

$$\zeta'' + \mathrm{Pr}\mathcal{F}\zeta' = 0,$$

$$\mathcal{F}(0) = 0, \mathcal{F}'(0) = 1, \zeta(0) = 1 \text{ and}$$

$$\mathcal{F}' \to c^{-1}, \zeta' \to 0 \text{ as } \mathcal{Y} \to \infty. \qquad (38)$$

Now using the regular perturbation expression of $\mathcal{F}$ and ζ as

$$\mathcal{F} = \mathcal{F}_0 + \frac{1}{c}\mathcal{F}_1 + \cdots,$$

$$\zeta = \zeta_0 + \frac{1}{c}\zeta_1 + \cdots , \qquad (39)$$

we have the leading order equations

$$\mathcal{F}_0''' + \lambda^*\mathcal{F}_0''\mathcal{F}_0''' + \mathcal{F}_0\mathcal{F}_0'' - \mathcal{F}_0'^2 = 0,$$

$$\zeta_0'' + \mathrm{Pr}\mathcal{F}_0\zeta_0' = 0,$$

$$\mathcal{F}_0(0) = 0, \mathcal{F}_0'(0) = 1, \zeta_0(0) = 1 \text{ and}$$

$$\mathcal{F}_0' \to 0, \zeta_0' \to 0 \text{ as } \mathcal{Y} \to \infty. \qquad (40)$$

By setting $\lambda^* = 0.5$ and $\mathrm{Pr} = 1$, a numerical solution of (40) gives $\mathcal{F}_0''(0) = -1.316134$ and $\zeta_0'(0) = -0.556919$, so that

$$F''(0) \sim -1.316134c^{\frac{3}{2}} + \cdots$$

$$\zeta'(0) \sim -0.556919c^{\frac{1}{2}} + \cdots \text{ for large } c. \quad (41)$$

To verify our analysis, we tabulated the values of $c^{-\frac{3}{2}}F''(0)$ and $c^{-\frac{1}{2}}\zeta'(0)$ against c in Table 1. We observe that as c increases, the solutions approach their respective asymptotic limits of -1.316134 and -0.556919.

Table 1: Asymptotic values of $c^{-3/2}F''(0)$ and $c^{-1/2}\zeta'(0)$

c	$F''(0)$	$\zeta'(0)$	$c^{-3/2}F''(0)$	$c^{-1/2}\zeta'(0)$
5	-12.984637	-1.359882	-1.161381	-0.608202
20	-115.56896	-2.542579	-1.292100	-0.568538
60	-608.62809	-4.342031	-1.309559	-0.560554
100	-1312.3680	-5.590453	-1.312368	-0.559045
200	-3117.4350	-7.890453	-1.314312	-0.557939
∞	-	-	-1.316134	-0.556919

6 Results and Discussion

To validate our results, we compare the values of $F''(0)$ (when non-Newtonian parameter $\lambda = 0$) on the stretching/shrinking sheet with Ishak et al. [13]. The detailed comparisons are in Table 2, displaying a strong concurrence between our results and the cited work. Also, the values of $F''(0)$ for λ =0.3 with different values of c are tabulated in Table 2. An increase in |c| leads to a decrease in the values of $F''(0)$ in the first solution, while it has the opposite effect in the second solution. In Table 2, $F''(0)$ gives two different values for some selected negative values of c, but after crossing the point -1, it provides only a single value. The point c_T connects both solution branches, and when $c \to -1$, no such critical point exists, and after crossing the point -1, it becomes a single branch. Our theoretical results are also closely connected with the above fact, as $c \to -1, F''(0) \geq 0$. If $F''(0) > 0$, then from (11), it is found that $F'''(0) = 0$. Consequently, $F''(0) = 0$, and all subsequent derivatives are zero at $s = 0$, which cannot satisfy the conditions $F'(0) = -1$ and $F'(\infty) \to 1$. Therefore, a unique solution exists when $c > -1$, and dual solutions occur for $c_T \leq c \leq -1$, and there is no solution for $c < c_T$. The critical point c_T for $\lambda = 0.1$ and 0.3 are -1.24701 and -1.24768 (see Figures 1-2). The solution domain expands with increasing λ, and c_T is more negative for the non-Newtonian case than the Newtonian case, highlighting that λ plays a significant role in the existence of solutions, as supported by theoretical results. Figure 3 demonstrates a significant decrease in the velocity profile $F'(s)$ with increasing λ for both solution branches. It is observed that the thickness of the momentum boundary layer is larger for Newtonian fluid than for non-Newtonian fluid.

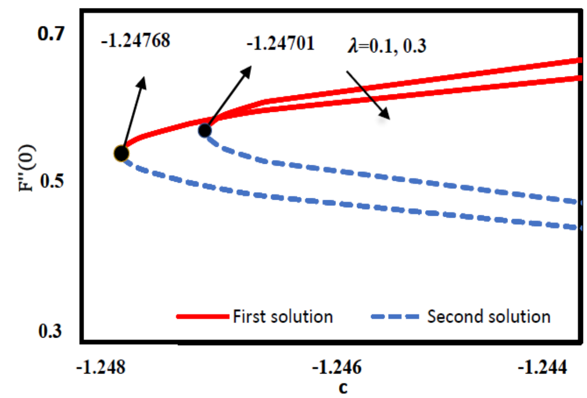

Figure 1. Effect of λ on $F''(0)$.

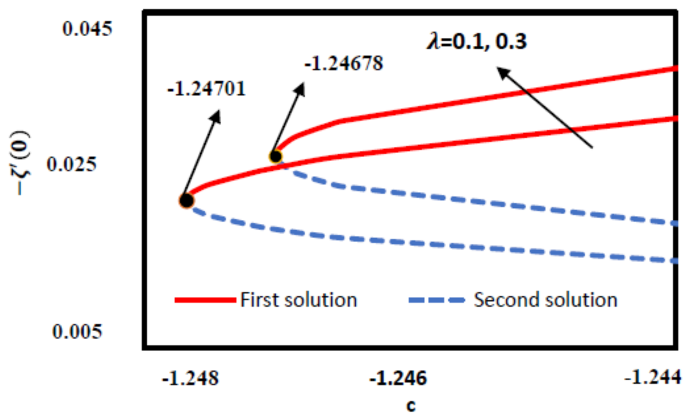

Figure 2. Effect of λ on $-\zeta'(0)$.

The temperature profile for both solutions increases with the non-Newtonian parameter λ (see Figure. 4), resulting in a rise in the thickness of the thermal boundary layer. Figure 5 shows that $F'(s)$ decreases in the first solution but increases in the second solution as $|c|$ increases. Conversely, $\zeta(s)$ increases with $|c|$ in the first solution, while decreasing in the second solution (see Figure 6). The momentum and thermal boundary layer thicknesses are found to be smaller in the first solution compared to the second solution. In Figure 7, $F(s)$ decreases in the first solution but increases in the second solution as $|c|$ increases. Initially, each curve shows a decline, reaching certain negative values for small s. However, these values gradually increase and become positive beyond a certain distance from the sheet.

Table 2. Comparison of $F''(0)$ for various values of λ and c.

λ	c	Present		Ishak [13]	
		First Solution	Second Solution	First Solution	Second Solution
0	-0.25	1.402240	-	1.402241	-
	-0.50	1.495669	-	1.495670	-
	-0.75	1.489298	-	1.489298	-
	-1	1.328816	0	1.328817	0
	-1.15	1.082231	0.116701	1.082231	0.116702
	-1.20	0.932473	0.233649	0.932474	0.233650
	-1.2465	0.584291	0.554281	0.584295	0.554283
0.3	-0.25	1.254506	-	-	-
	-0.75	1.321493	-	-	-
	-0.9	1.262148	-	-	-
	-1	1.187971	0	-	-
	-1.12	1.036961	0.064495	-	-
	-1.18	0.911318	0.163578	-	-
	-1.22	0.778358	0.283952	-	-
	-1.24765	0.536212	0.519569	-	-
	-1.24768	0.528127	0.528547	-	-

Table 3: Smallest eigenvalues for different λ

λ	c	First solution	Second solution
0.1	-1.24	0.157272	-0.258123
	-1.19	0.573241	-0.598794
	-1.18	0.627739	-0.638914
0.3	-1.24	0.016590	-0.348644
	-1.21	0.341042	-0.571240
	-1.20	0.405736	-0.618171

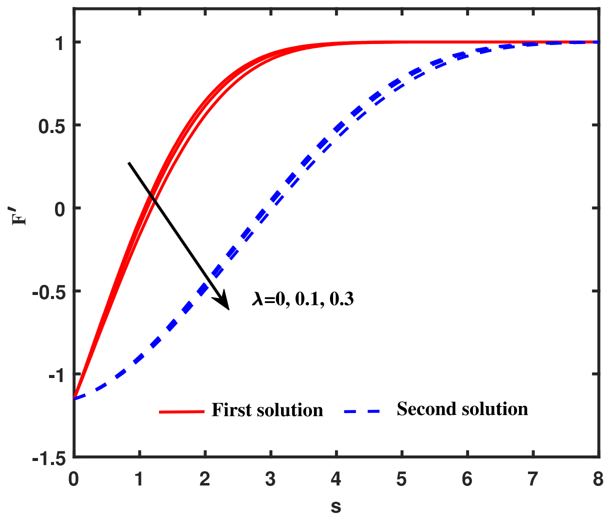

Figure. 3: Effect of λ on $F'(s)$.

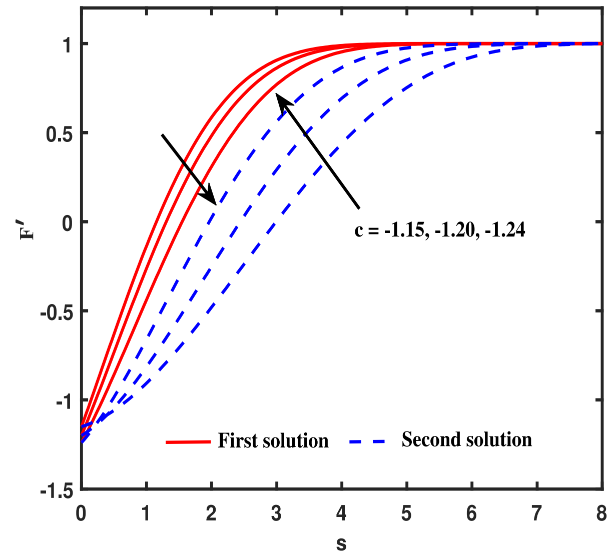

Figure. 5: Effect of c on $F'(s)$.

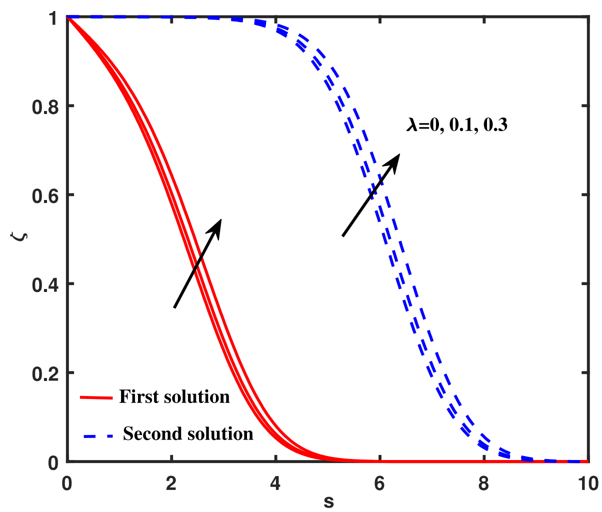

Figure. 4: Effect of λ on $\zeta(s)$.

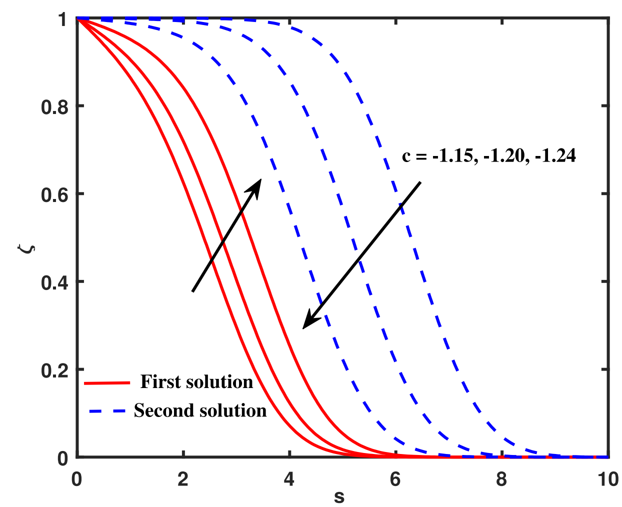

Figure. 6: Effect of c on $\zeta(s)$.

The stability analysis is performed using the BVP4C function in MATLAB software. The detailed procedure and calculation are mentioned in Appendix A. As shown in Table 3, the smallest eigenvalues for both solutions are computed numerically for different shrinking parameters c. In the first solution, the eigenvalues are observed to be real and positive, while in the second solution, they are negative. Because of the positive smallest eigenvalues, initial disturbances in the

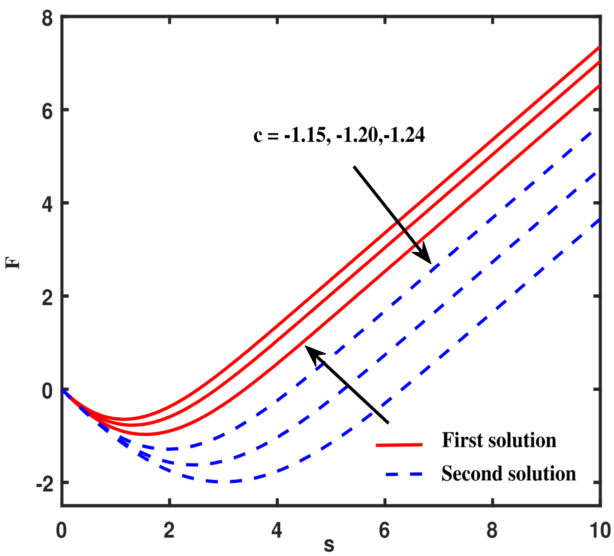

Figure. 7: Effect of c on $F(s)$.

fluid flow diminishes over time, that is $e^{-\omega\epsilon} \to 0$ as $\epsilon \to \infty$. Consequently, the first solutions are determined to be stable. However, the smallest negative eigenvalue suggests an amplification of initial disturbances in the flow, given by $e^{-\omega\,\epsilon} \to \infty$ indicating that the flow solutions (second solution) exhibit unstable behavior. The stable solution is physically meaningful for the above flow, whereas the unstable solution is not.

7 Conclusion

The research delved into the boundary layer stagnation-point flow and convective heat transfer on a linearly stretching/shrinking surface in non-Newtonian Williamson fluid. A suitable similarity transformation is employed to convert the PDEs into nonlinear ODEs for modelling purposes. The application of the shooting method illustrates the existence of a solution and examines its characteristics. The numerical solution for this study is acquired by implementing the shooting-based numerical code in MATLAB, specifically using the BVP4C solver. Furthermore, a connection has been established between theoretical results and numerical investigations. A temporal stability analysis is conducted to identify a stable solution, providing insight into the primary flow dynamics. The main findings of this study can be outlined as follows

- The existence of a unique solution to the nonlinear equation is proved for the stretching/shrinking parameter $c \in (-1, \infty)$.
- Dual solutions exist for c $\in [c_T, -1]$, and there does not exist any solution for $c \in (-\infty, c_T)$.
- The velocity profile $F'(s)$ decreases with non-Newtonian parameter λ in both solution branches, whereas the temperature profile $\zeta(s)$ increases with λ.
- In the first solution branch, the boundary layer thickness (for both momentum and thermal) is smaller compared to the second solution branch. Additionally, the solution domain expands with increasing λ.
- Stability analysis indicates that the first solution branch is physically acceptable, as all the smallest eigenvalues are positive, whereas the second solution branch is unstable.
- An asymptotic solution for large $c > 0$ shows that the expressions $F''(0) \sim -1.316134\, c^{3/2}$ and $\zeta'(0) \sim -0.556919\, c^{1/2}$ as $c \to \infty$.

Appendix A

A study on temporal stability is conducted using the foundational research of Merkin [16], who identified potential practical unreliability in the lower branch. To achieve this, we consider the time-varying representation of equations (11)-(12)

$$\left(\frac{\partial u}{\partial t} + v\frac{\partial u}{\partial y} + u\frac{\partial u}{\partial x}\right) = \frac{\mu_0}{\rho}\left(\frac{\partial^2 u}{\partial y^2} + 2\Gamma\frac{\partial u}{\partial y}\frac{\partial^2 u}{\partial y^2}\right)$$

$$-\frac{1}{\rho}\frac{\partial p}{\partial x},$$

$$\left(\frac{\partial T}{\partial t} + v\frac{\partial T}{\partial y} + u\frac{\partial T}{\partial x}\right) = \frac{k}{\rho c_p}\frac{\partial^2 T}{\partial y^2}. \qquad (A1)$$

Due to the presence of a time variable, we introduce the following new dimensionless variable

$$v = bxF'(s,\epsilon), v = -\sqrt{b\nu}F(s,\epsilon), T = T_w + (T_w - T_\infty)\zeta(s,\epsilon), \text{ and } \epsilon = bt, \text{ where } s = \sqrt{\frac{b}{\nu}}y. \qquad (A2)$$

Here, ϵ represents the updated non-dimensional time parameter. Employing ϵ refers to an initial value challenge, raising the query of which solution holds physical validity. By using (A2), from (A1), we get

$$F''' + 1 + \lambda F''F''' + FF'' - F^2 - F'_\epsilon = 0,$$
$$\zeta'' + \Pr F\zeta' - \Pr\zeta_\epsilon = 0, \qquad (A3)$$

where, $'$ denotes the derivative concerning s and superscript ϵ represents derivative with respect to ϵ. The boundary conditions for the above time dependent flow are

$$F(0,\epsilon) = 0, F'(0,\epsilon) = c, F'(\infty,\epsilon) \to 1, \zeta(0,\epsilon) = 1, \zeta(\infty,\epsilon) \to 0. \qquad (A4)$$

To assess the stability of the steady flow solution, $F(s) = F_0$ and $\zeta(s) = \zeta_0$ satisfy equations (11)-(12), a group of perturbed equations is examined to facilitate the separation of variables

$$F(s,\epsilon) = F_0(s) + e^{-\omega\epsilon}M(s,\epsilon), \zeta(s,\epsilon) = \zeta_0(s) + e^{-\omega\epsilon}N(s,\epsilon)\,. \qquad (A5)$$

Here, ω is an unknown eigenvalue, and both $F(s,\epsilon)$ and $\zeta(s,\epsilon)$ are significantly smaller than F_0 and ζ_0. Solving the eigenvalue problem (A4)-(A5) provides a series of eigenvalues $\omega_1 < \omega_2 < \omega_3 < \cdots$. If ω_1 is negative, it implies initial disturbance growth, indicating flow instability. Conversely, when w_1 is positive, there is initial decay, signifying flow stability. Substituting (A5) into (A3)-(A4) and leads to the following linearized problem

$$M''' + \lambda F_0''M''' + \lambda F_0'''M'' - 2F_0'M' + F_0M'' + MF_0''$$
$$+\omega M' - M'_\epsilon = 0,$$
$$\frac{1}{Pr}N'' + F_0N' + M\zeta_0' + \omega N - N_\epsilon = 0,$$
$$M(0,\epsilon) = 0, M'(0,\epsilon) = 0, N(0,\epsilon) = 0,$$
$$M'(\infty,\epsilon) \to 0, N(\infty,\epsilon) \to 0. \qquad (A6)$$

Now, we are putting $\epsilon = 0$ for check the stability of steady state solution and considering $M(s,0) = M_0(s)$ and $N(s,0) = N_0(s)$, then equations (A6) become

$$M_0''' + \lambda F_0''M_0''' + \lambda F_0'''M_0'' - 2F_0'M_0' + F_0M_0''$$
$$+M_0F_0'' + \omega M_0' = 0,$$
$$\frac{1}{Pr}N_0'' + F_0N_0' + M_0\zeta_0' + \omega N_0 = 0,$$
$$M_0(0) = 0, M_0'(0) = 0, N_0(0) = 0, M_0'(\infty) \to 0,$$
$$N_0(\infty) \to 0. \qquad (A7)$$

Solving equations (A7) numerically, one can easily get the smallest eigenvalue. See [24] for a detailed explanation of determining the smallest eigenvalue. To solve it, we need an additional boundary condition. Therefore, without loss of generality, we take $M_0''(0) = 1$.

References

[1] Chhabra R P (2010) non-Newtonian fluids: an introduction. Rheology of complex fluids pp.3-34.

[2] Irgens F (2014) Rheology and non-Newtonian fluids, vol. 190 Springer.

[3] Williamson R V (1929) The flow of pseudoplastic materials. Industrial & Engineering Chemistry 21(11), 1108-1111.

[4] Lyubimov D, Perminov A (2002) Motion of a thin oblique layer of a pseudoplastic fluid. Journal of Engineering Physics and Thermophysics 75(4), 920-924.

[5] Nadeem S, Ashiq S and Ali M (2012) Williamson fluid model for the peristaltic flow of chyme in small intestine. Mathematical Problems in Engineering.

[6] Akbar N S (2015) Mixed convection analysis for blood flow through arteries on Williamson fluid model. International Journal of Biomathematics 8(04), 1550045.

[7] Khan N A, Khan H (2014) A boundary layer flows of non-Newtonian Williamson fluid. Nonlinear Engineering 3(2), 107-115.

[8] Nadeem S, Hussain S (2014) Heat transfer analysis of Williamson fluid over exponentially stretching surface. Applied Mathematics and Mechanics 35(4), 489-502.

[9] Hamid A, Khan M and Khan U (2018) Thermal radiation effects on Williamson fluid flow due to an expanding/contracting cylinder with nanomaterials: dual solutions. Physics Letters A 382(30), 1982-1991.

[10] Paullet J, Weidman P (2007) Analysis of stagnation point flow toward a stretching sheet. International Journal of Non-Linear Mechanics 42(9), 1084-1091.

[11] Wang C (2008) Stagnation flow towards a shrinking sheet. International Journal of Nonlinear Mechanics 43(5), 377-382.

[12] Crane L J (1970) Flow past a stretching plate. Zeitschrift f"ur angewandte Mathematik und Physik ZAMP 21, 645-647.

[13] Ishak A, Lok Y Y and Pop I (2010) Stagnation point flow over a shrinking sheet in a micropolar fluid. Chemical Engineering Communications 197(11), 1417-1427.
[14] Sarkar G M, Sahoo B (2020) Dual solutions of magnetohydrodynamic boundary layer flow and a linear temporal stability analysis. Proceedings of the Institution of Mechanical Engineers, Part E: Journal of Process Mechanical Engineering 234(6), 553-561.
[15] Haq R U, Zahoor Z and Shah S S (2023) Existence of dual solution for MHD boundary layer flow over a stretching/shrinking surface in the presence of thermal radiation and porous media: KKL nanofluid model. Heliyon 9(11).
[16] Merkin J (1986) On dual solutions occurring in mixed convection in a porous medium. Journal of engineering Mathematics 20(2), 171-179.
[17] Roy N C, Pop I (2023) Dual solutions of a nanofluid flow past a convectively heated nonlinearly shrinking sheet. Chinese Journal of Physics 82, 31-40.
[18] Usafzai W K, Pop I and Revnic C (2024) Dual solutions for the two-dimension copper oxide with silver (CuO-Ag) and zinc oxide with silver (Zno-Ag) hybrid nanofluid flow past a permeable shrinking sheet in a dusty fluid with velocity slip. International Journal of Numerical Methods for Heat & Fluid Flow 34(1), 259-279.
[19] Miklavcic M, Wang C (2006) Viscous flow due to a shrinking sheet. Quarterly of Applied Mathematics 64(2), 283-290.
[20] Van Gorder R A, Vajravelu K and Pop I (2012) Hydromagnetic stagnation point flow of a viscous fluid over a stretching or shrinking sheet. Meccanica 47(1), 31-50.
[21] Sarkar G M, Sarkar S and Sahoo B (2022) Analysis of Hiemenz flow of Reiner-Rivlin fluid over a stretching/shrinking sheet. World Journal of Engineering 19(4), 522-531.
[22] Abdal S, Hussain S, Siddique I, Ahmadian A and Ferrara M (2021) On solution existence of MHD Casson nanofluid transportation across an extending cylinder through porous media and evaluation of priori bounds. Scientific Reports 11(1), 7799.
[23] Mondal, D., Pandey, A. K., & Das, A. (2025). Flow and heat transfer analysis of an ionanofluid above a rotating disk undergoing torsion. Chinese Journal of Physics, *93*, 127-157.
[24] Mondal, D., Das, A., & Pandey, A. K. (2025). Existence and nonuniqueness of solutions for flow driven by a revolving hybrid nanofluid above a stationary disk. Journal of Mathematical Analysis and Applications, 129743